Metallurgical and Materials Applications of
Shock-Wave and High-Strain-Rate Phenomena
L.E. Murr, K.P. Staudhammer and M.A. Meyers (Editors)

59

High-strain-rate behavior of pure tantalum in explosively formed penetrator and shaped charge regimes

S. Pappu, C-S. Niou, C. Kennedy, L. E. Murr, L. DuPlessis, and M. A. Meyers*

Department of Metallurgical and Materials Engineering and Materials Research Institute, The University of Texas at El Paso, El Paso, TX 79968

*Department of AMES, University of California, San Diego, La Jolla, CA 92093

In this paper, we have analyzed and compared the microstructures and microstructural evolution in explosively formed penetrator (EFP) and shaped charge slugs using optical microscopy, TEM and microhardness testing. We also characterized a plane-wave shock-loaded Ta since this is a precursor to these regimes. Dynamic recovery (DRV) and dynamic recrystallization (DRX) play an important role in the evolution of the microstructure in these regimes. TEM images show a range of dislocation features consistent with low-energy dislocation structures (LEDS). Twins were clearly seen in shock-loaded Ta at a peak pressure of 45 GPa but not in the residual EFP and shaped charge components.

1. INTRODUCTION

Significant progress has been made in recent years in understanding the complex phenomena underlying the high-strain-rate regimes of shaped charges, EFPs and shock-loading. A great deal of information has been generated by Murr and co-workers [1-6], Meyers *et al.* [7, 8], Zernow [9], and others. But the sheer number of parameters involved, e.g., shock front morphology, peak shock pressure, pulse duration, initial liner microstructure, strain rate, strain state etc., and lack of sufficient temperature and strain profiles across the cross-sections make these systems extremely complex and the microstructural features intriguing.

In this investigation, we have addressed some of the issues involved in the microstructural evolution in pure Ta shaped charges, EFPs, and plane-wave shock-loaded specimens, all of which are sequentially influenced by a strong shock-wave generated by a high-explosive (H.E.) detonation.

2. EXPERIMENTAL DETAILS

Optical microscopy, microhardness testing, and TEM (using a 200kV Hitachi-8000 STEM) studies were carried out on annealed Ta shaped charge and EFP starting liners and the corresponding soft-recovered slugs. Light and thin-foil electron microscopy were also done on a

plane-wave shock-loaded specimen subjected to a peak shock pressure of 45 GPa and a pulse duration of 2μs.

The etching solution for optical metallography consisted of 1 part HNO_3, 2 parts HCl and 4 parts HF. The temperature for etching was 0°C. The loads used for Vickers microhardness testing were 100gf (0.5N). Jet polishing was done on 3mm discs ground to a thickness of approximately 150μm, using a Struers Tenupol III jet polisher. The jet polishing solution consisted of 750ml CH_3OH, 150ml glycerin, 135ml H_2SO_4, 75ml HF and 350ml C_2H_5OH. Methanol and glycerin were first mixed and cooled to −20°C. Sulfuric acid was added to this mixture very slowly and the resulting solution cooled to −10°C. Finally hydrofluoric acid and ethanol were added; temperature used for jet polishing was approximately 8-9°C at a voltage which was gradually decreased from 12V to 8V for the preparation of each sample.

3. RESULTS AND DISCUSSION

Figure 1 depicts the formation of a shaped charge slug and particulating jet and an EFP slug as a result of a strong shock-wave generated by H.E. detonations behind the starting liners. It can clearly be seen from the figure that the differences in liner geometry lead to different shock-wave-liner interactions resulting in the formation of different end-structures. The formation of these products is explained in greater detail elsewhere [1, 10]. Whereas the shaped charge jets experience strains in excess of 1000% at strain rates of 10^6 s^{-1} or greater, the EFP experiences non-uniform strains of much lower magnitude (about 300%) [4].

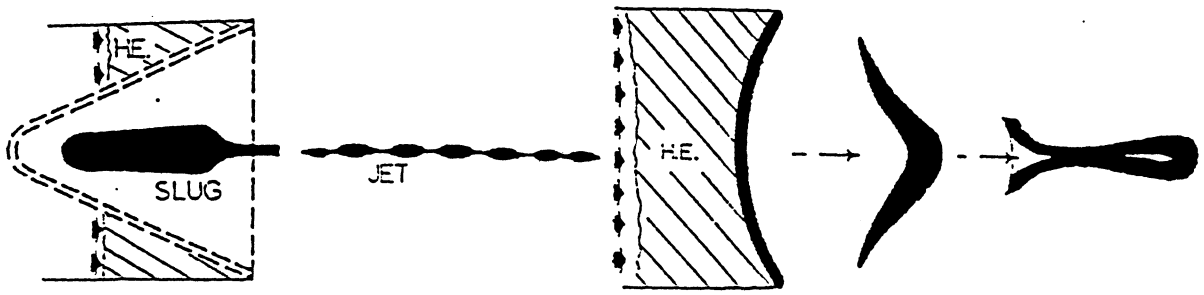

(a) (b)

Figure 1. Schematic showing the formation of (a) shaped charge slug and particulating jet, and (b) EFP slug. Note the difference in the angle at which the shock-front intercepts the liners in the two systems.

Figure 2 illustrates the optical and TEM images of the starting shaped charge and EFP liners. The optical micrographs show generally equiaxed grains and the TEM views show the dislocation distribution and loops inside these grains. The grain size of both the shaped charge and the EFP starting liners is approximately 53μm (corresponding to an average intercept length ($\bar{l}$) of 35μm).

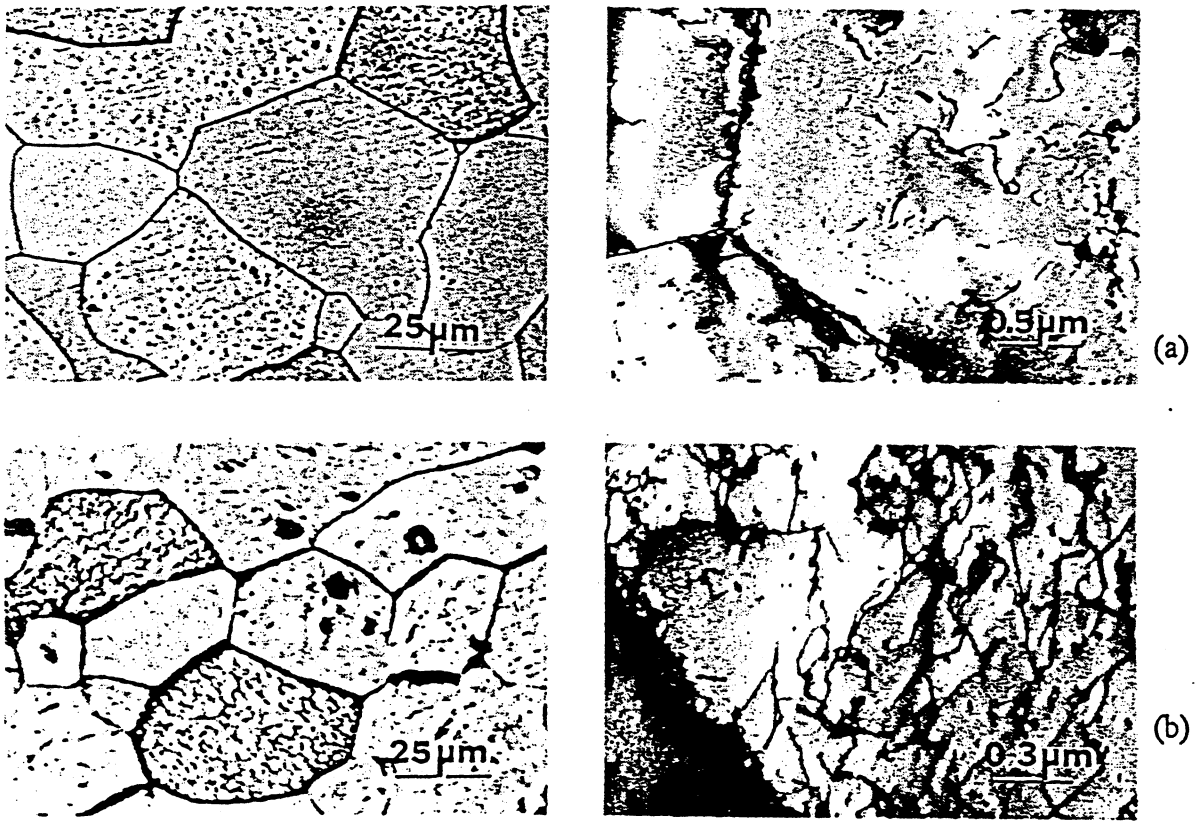

Figure 2. Optical (left) and TEM (right) views of (a) shaped charge liner cone showing uniform distribution of dislocations inside equiaxed grains, and (b) EFP liner showing numerous dislocation loops in generally equiaxed grains.

Figure 3 shows optical micrographs of the various zones of shaped charge and EFP slugs. The shaped charge slug microstructure is characterized by concentric zones showing small, equiaxed grains in the central core region which evolve into elongated, wavy structures as the distance from the center increases. The equiaxed grains in the center have an average diameter of 0.53μm ($\bar{l}$=0.35μm), a reduction by 2 orders of magnitude over the initial liner grain size. In addition, the shaped charge slug center is about 40% less harder than the zone of maximum hardness and is also considerably softer than the rest of the slug [Figure 4(a)]. These observations are strongly indicative of DRX.

The EFP microstructures, as shown in Figure 3(b), vary from some reasonably equiaxed and lightly deformed regions near the tail section to severely deformed regions in the center and near the head. These microstructures bear some resemblance to the shaped charge slug microstructures but vary throughout the EFP geometry in consonance with the variation in strains and temperatures within the system. There is also a preponderance of what appears to be DRV in heavily deformed EFP regions, in contrast to recrystallized or subgrain microstructures.

The variation in microhardness with distance from the shaped charge slug center and the zones of different average microhardness values along the EFP half-section are illustrated in Figure 4. It is interesting to note that the shaped charge slug center, in spite of having smaller grains, is considerably softer than the edge (127 VHN versus 197 VHN). This "inversion" effect strongly

favors the arguments for DRX, as noted above, and is a result of the reduction in dislocation density. The center, however, is harder than the liner cone (127 VHN versus 109 VHN) and this feature is due to the drastic reduction in grain size. Likewise, the heavily deformed zones of the EFP are relatively softer (167-187 VHN) than the lightly deformed ones (179-199 VHN) and are suggestive of DRV and possibly some DRX, as noted earlier.

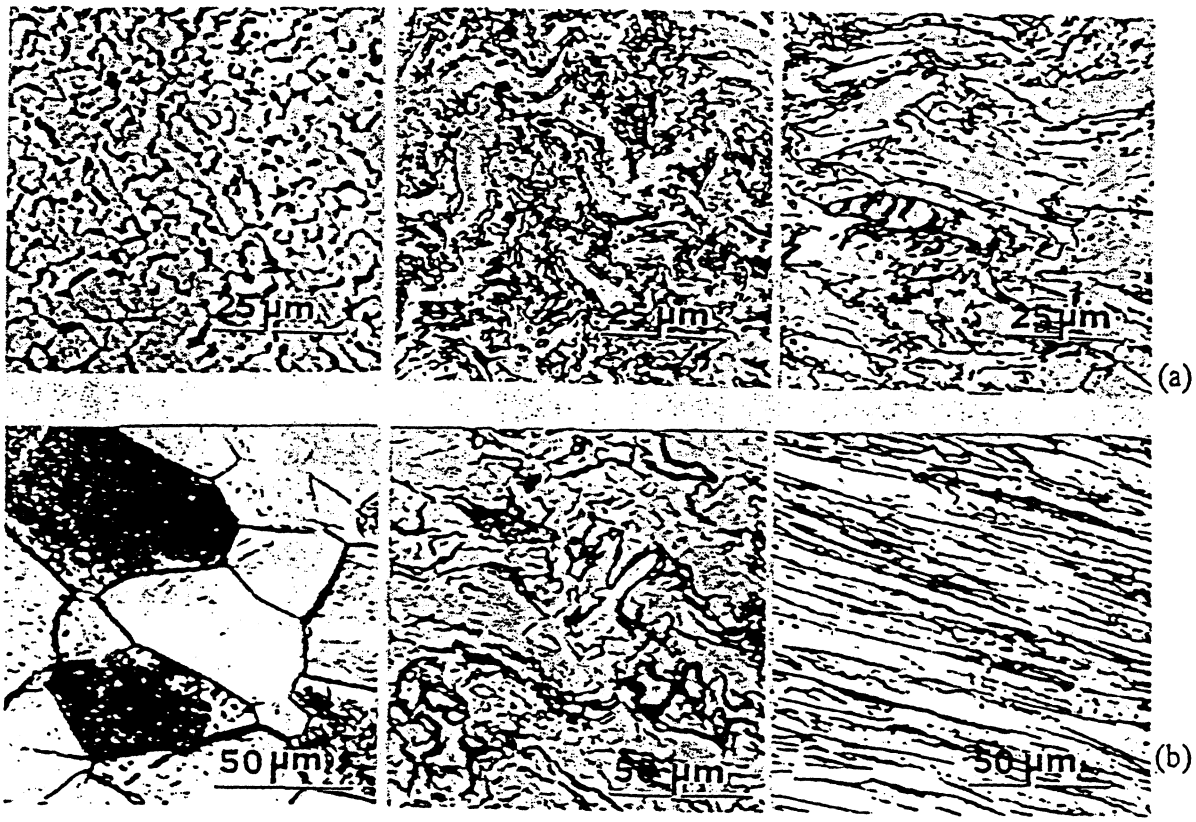

Figure 3. Light micrographs showing the different zones of microstructural evolution in (a) shaped charge slug, and (b) EFP.

Figure 5 shows TEM images of the zones of the shaped charge and EFP slugs having equiaxed and elongated structures. The central zone of the shaped charge slug contains a very small core of larger, recrystallized grains surrounded by very small grains and subgrains which evolve into elongated, wavy grains having low-angle (~2°) sub-boundaries, as shown in Figure 5(b). These sub-boundaries are the result of the DRV process. Thus, the shaped charge slug is characterized by a zone of DRV near the edge and by one of DRX at the center.

The TEM image of the EFP near the tail shows fairly equiaxed grains, though they look clearly distorted when compared with the starting equiaxed liner plate. The microstructures show subgrains with the accompanying SAD pattern showing misorientations of about 9°. This suggests occurrence of some DRX. The grain boundary structures are also well-developed and are representative of general high-angle boundaries. The TEM image of the heavily deformed zone near the EFP head shows a mixture of subgrains and dislocation cells (including elongated cells). In the evolution of microstructure in both the shaped charge and the EFP, these elongated cells appear to "break up" into appropriately misoriented subgrains or cell blocks (CBs).

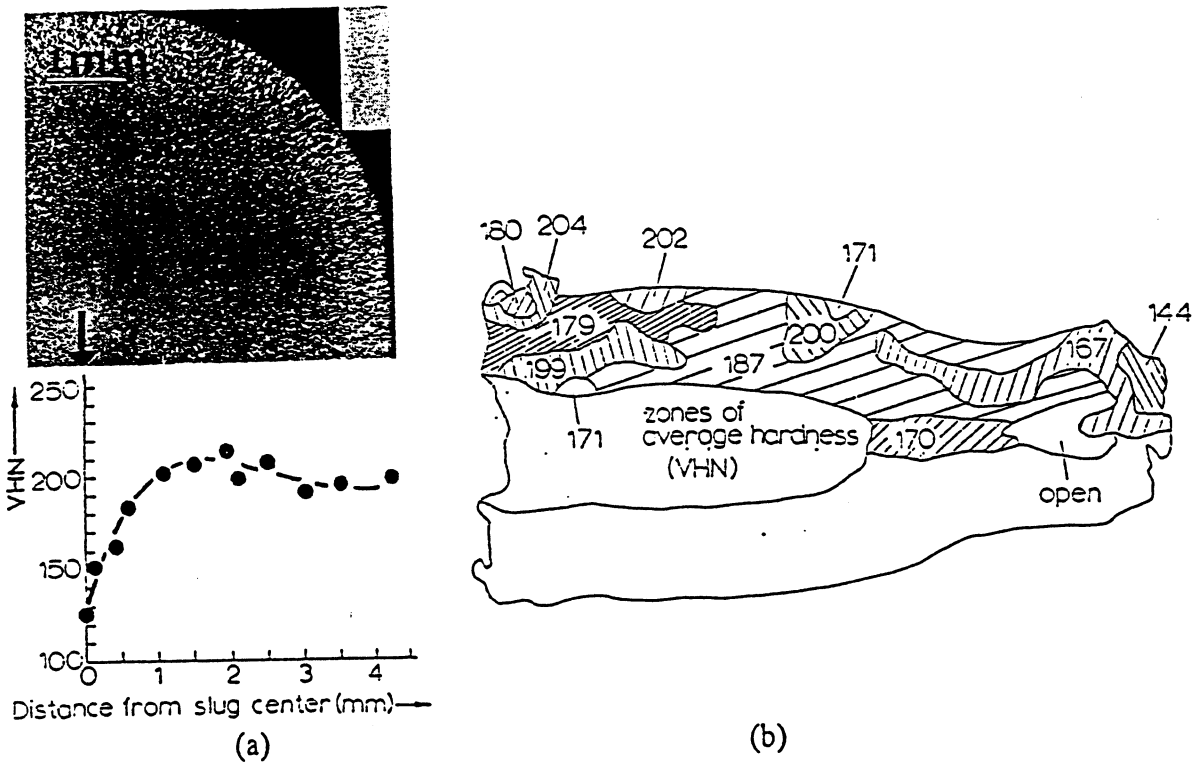

Figure 4. Microhardness variations in (a) shaped charge slug (after ref. [5]), and (b) EFP slug.

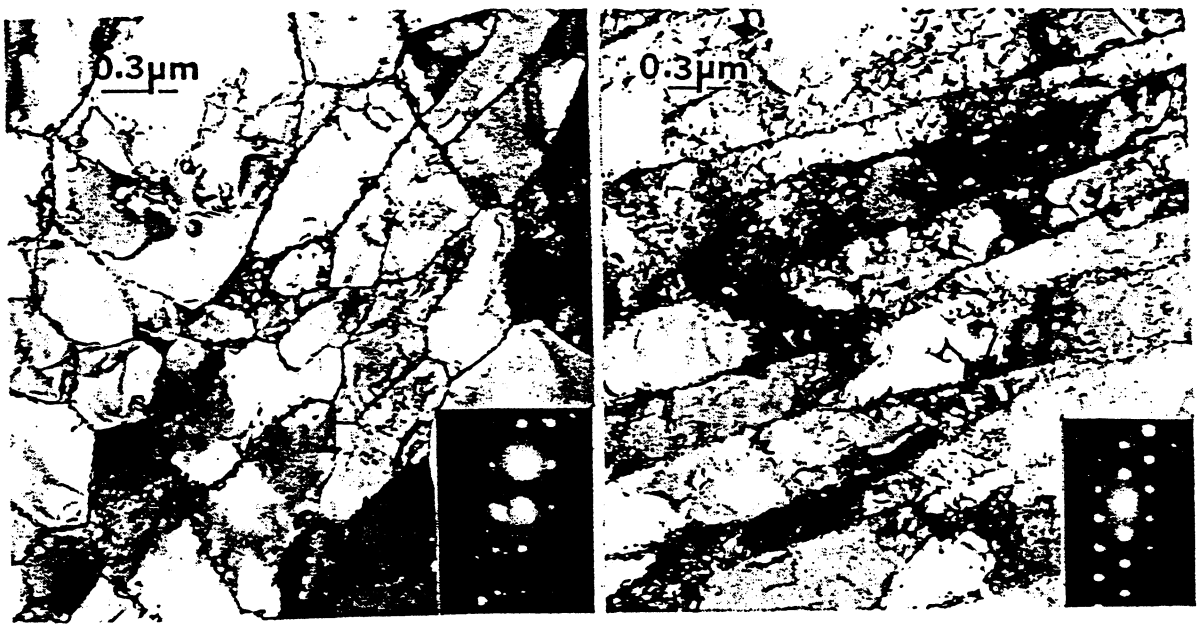

Figure 5. TEM images showing (a) equiaxed grains in the central region of the shaped charge slug, (b) elongated grains and corresponding SAD pattern away from the central region of the shaped charge slug.

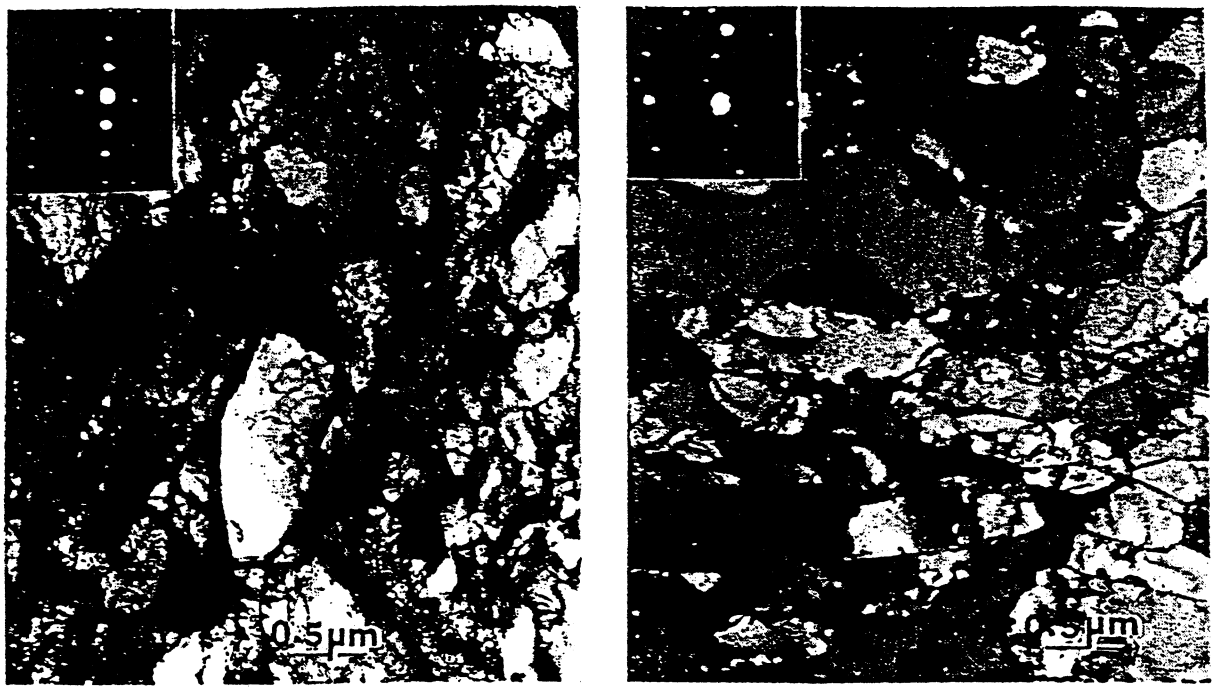

(c) (d)

Figure 5 (cont.). TEM images showing (c) fairly equiaxed grains near the EFP tail, and (d) mixtures of dislocation cells and subgrains in the heavily deformed regions near the EFP head.

The dislocation tangles in low strain regions of the above microstructures lead to cell structures which decrease in size, elongate and eventually break up into very fine CBs. Among the neighboring CBs, the simultaneously acting slip systems differ, resulting in straining which causes lattice rotation from CB to CB. With such refinement in microstructure, the relative boundary misorientations increase. In heavily strained regions containing very fine CBs, orientations differ markedly rendering a virtual grain refinement. These microstructural features and evolution, observed in varying proportions in both the shaped charges and the EFPs, are characterized by DRV and, in extreme cases, by DRX. These features are also consistent with the LEDS theory [5, 11], according to which the application of the second law of thermodynamics requires the dislocation structures to attain minimum energy configurations subject to limitations of slip systems and dislocation mobility.

Figure 6 shows optical and TEM images of a Ta specimen subjected to a plane shock wave of about 45 GPa peak pressure and 2μs pulse duration. The twins, shown here in a (100) grain, occur in 4 different <042> directions corresponding to traces of {112} planes, which are preferred for twinning in BCC materials. The dark-field image is obtained utilizing the twin reflections shown circled in the SAD pattern. Additional details of twins in shocked Ta are included in a recent article by Murr *et al.* [12].

It is interesting to note that neither the shaped charge components nor the EFP slug show any trace of deformation twins. Twinning is a process which occurs only if pressure, shear stresses and temperature can reach together the required threshold conditions [13]. In addition, crystallographic direction, incubation time of twinning, pulse duration, existing substructure and the grain size can

also alter these conditions. Based on an earlier study [14] and present observations, it can be predicted that a peak pressure of at least about 25 GPa is necessary for twinning in Ta. The absence of any twins in the EFP could be attributed to the non-attainment of similar pressures. Though the shaped charge slug and jet experience much greater pressures (upto 100 GPa), the twins are still not observed. This is due to the post-shock deformation which completely obliterates any twins which might have nucleated.

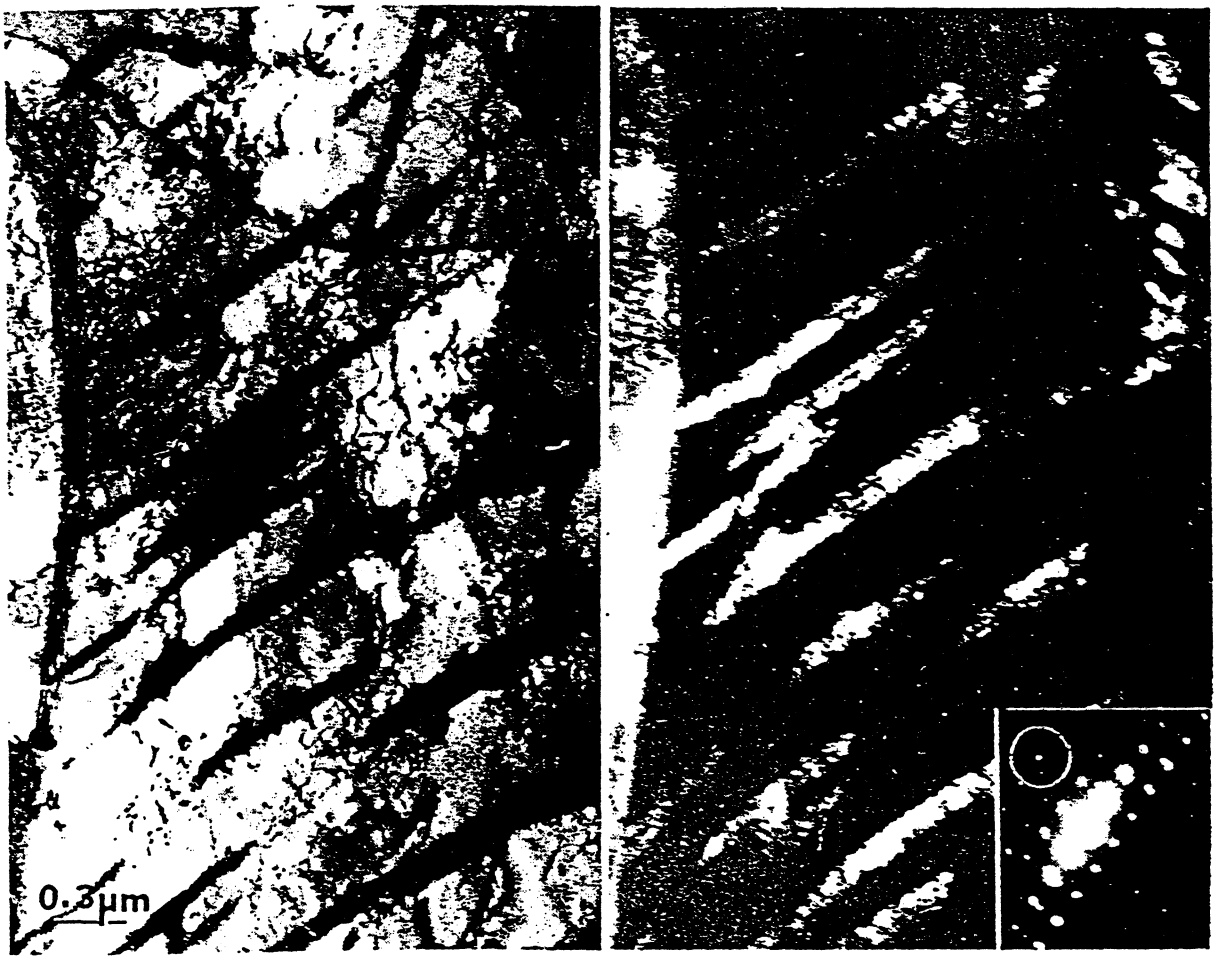

Figure 6. Optical and bright and dark-field TEM images showing twins in a shock-loaded Ta specimen. Grain surface orientation is (100). Twins occur on {112} planes in the <042> directions.

4. SUMMARY AND CONCLUSIONS

DRV and DRX play an important role in the microstructural evolution of the shaped charge and EFP slugs. The shaped charge slug showed concentric regions consisting of a central zone of small, equiaxed grains which evolve into elongated subgrains and wavy structures with increasing distance from the center. The final grain size in the slug was two orders of magnitude smaller than that in the liner cone, a strong indication that DRX is a prominent participating phenomenon. The evidence in favor of DRX is reinforced by the significant softening of the slug center compared to the exterior,

in spite of it having much smaller grains. The TEM images showed a wide range of microstructural features including dislocation cells, dense dislocation walls, regular grain boundaries and sub-boundaries, consistent with the LEDS theory [5, 11].

The EFP microstructures showed features similar to those observed in the shaped charge slug with most variations and evolution suggestive of DRV, and, in extreme cases, by DRX.

Evidence for deformation twinning was presented in a plane-wave shock-loaded Ta subjected to a peak pressure of about 45 GPa with a 2μs pulse duration. Insufficient peak pressures in the EFP, and twin obliteration due to post-shock deformation in shaped charge components explain the absence of any twins in these regimes. Although it is not known whether deformation twins contribute significantly to the actual self-forming processes, it seems unlikely they have any effect in Ta EFP formation since they are apparently not generated by the shock precursor [Figure 1(b)].

ACKNOWLEDGEMENTS

This research was supported in part by a Mr. and Mrs. MacIntosh Murchison Endowed Chair and U.S. Army Contract DAAA21-94-C-0059.

REFERENCES

1. L. E. Murr, H. K. Shih, C-S. Niou and L. Zernow, Scripta Met. et Mater., 29 (1993) 567-572
2. L. E. Murr, C-S. Niou, J. C. Sanchez and L. Zernow, ibid., 32:1 (1995) 31-36
3. C-S. Niou, L. E. Murr, C. Feng and S. Pappu, Microstructural Science, 22 (1995) 73-85
4. L. E. Murr, C-S. Niou, H. K. Shih, J. A. Sanchez, S. Pappu and C. Feng, in: Proceedings of XVI Encuentro de Investigacion Metalurgica y I Congreso Internacional en Materiales, October 5-7, 1994, Instituto Tecnologico de Saltillo, Saltillo, Mexico, pp. 637-658
5. L. E. Murr, C-S. Niou, S. Pappu, J. M. Rivas and S. A. Quinones, Phys. Stat. Sol. (a), 149 (1995) 253-274
6. L. E. Murr, C-S. Niou, J. C. Sanchez, H. K. Shih, L. DuPlessis, S. Pappu and L. Zernow, J. Mater. Sci., 30 (1995) 2747-2758
7. M. A. Meyers, L. W. Meyer, J. Beatty, U. Andrade, K. S. Vecchio and A. H. Chokshi, in: Shock-Wave and High-Strain-Rate Phenomena in Materials, M. A. Meyers, L. E. Murr and K. P. Staudhammer, eds., Marcel-Dekker, NY, 1992, p. 529
8. U. Andrade, M. A. Meyers, K. S. Vecchio and A. H. Chokshi, Acta Metall. et Mater., 42:9 (1994) 3183-3195
9. L. Zernow, Proc. Tenth Int. Symp. on Ballistics (Vol.II), Oct. 1987 (ADPA)
10. M. A. Meyers, Dynamic Behavior of Materials, John Wiley and Sons, Inc., NY, 1994, p. 570
11. D. Kuhlmann-Wilsdorf, Phys. Stat. Sol. (a), 104 (1987) 121
12. L. E. Murr, C-S. Niou, E. Ferreyra T., S. Pappu, C. Kennedy, S. A. Quinones, J. M. Rivas, R. J. Romero and J. G. Maldonado, Multi-Dimensional Microanalysis in Materials Characterization: Some Case Examples, to be published in Microstructural Science, 23 (1996)
13. C. Y. Chiem, in: Shock-Wave and High-Strain-Rate Phenomena in Materials, M. A. Meyers, L. E. Murr and K. P. Staudhammer, eds., Marcel-Dekker, Inc., NY, 1992, p. 69
14. C. L. Wittman, R. K. Garrett, Jr., J. B. Clark and C. M. Lopatin, ibid., p.925